CO$_2$ Footprint of Thermal Versus Photothermal CO$_2$ Catalysis

Shenghua Wang, Athanasios A. Tountas, Wangbo Pan, Jianjiang Zhao, Le He, Wei Sun,* Deren Yang,* and Geoffrey A. Ozin*

Transformation of CO$_2$ into value-added products via photothermal catalysis has become an increasingly popular route to help ameliorate the energy and environmental crisis derived from the continuing use of fossil fuels, as it can integrate light into well-established thermocatalysis processes. The question however remains whether negative CO$_2$ emission could be achieved through photothermal catalytic reactions performed in facilities driven by electricity mainly derived from fossil energy. Herein, we propose universal equations that describe net CO$_2$ emissions generated from operating thermocatalysis and photothermal reverse water–gas shift (RWGS) and Sabatier processes for batch and flow reactors. With these reactions as archetype model systems, the factors that will determine the final amount of effluent CO$_2$ can be determined. The results of this study could provide useful guidelines for the future development of photothermal catalytic systems for CO$_2$ reduction.

1. Introduction

The rapid consumption of fossil fuels has led to serious energy, global warming, and ocean acidification crises, which poses a looming threat to the survival of humankind.[1] Chemical transformation of CO$_2$ into CO and CH$_4$ can help solve this problem.[2] Thermocatalysis,[3] electrocatalysis,[4] photocatalysis,[5] and, most recently, photothermal catalysis[6] have been demonstrated to be effective strategies to enable the reduction of CO$_2$ to value-added chemicals. Power used in these catalytic processes has often been provided by fossil-fuel-generated electricity. Light sources for enabling photocatalysis and photothermal catalysis employ electrically powered lamps, light-emitting diodes, and

lasers. This begs the question of whether a negative CO$_2$ footprint can be achieved in practice through light-assisted gas-phase heterogeneous catalysis ultimately powered by electricity.

Chen and co-workers recently studied the CO$_2$ footprint associated with the production of methanol via thermocatalysis, electrocatalysis and a hybrid of these two using CO$_2$ as the carbon source.[7] Surprisingly, their results indicate that in an ideal catalytic process, a net reduction of CO$_2$ can be achieved when the source of electricity emits less than 0.2 kg of CO$_2$ per kWh, a demanding metric to accomplish with current energy conversion systems. It was also found that a hybrid thermocatalysis and electrocatalysis system has the greater potential to transform CO$_2$ into methanol on the premise that the reaction rate could reach two orders of magnitude larger than what is currently achieved under laboratory conditions.[7]

These results reinforce the notion that it remains a challenge to realize negative CO$_2$ emission through thermocatalysis and electrocatalysis alone. In recent years, photothermal catalysis, a thriving route for CO$_2$ reduction with the aid of light in lieu of inputting intense heat, has prompted considerable interest. The reaction mechanism and reactor setup of photothermal catalysis can be established but also upgraded from the existing thermocatalysis, with the production rate achieving the magnitude of mol·g^{-1}·h^{-1} which is also comparable to that in thermocatalysis.[8] Combined with the development of photothermal reactors and solar concentrators, the industrialization of photothermal catalysis upon the existing infrastructure of thermocatalysis is promising. Moreover, the introduction of light can in some cases alter the reaction pathways, providing a simple and novel route to tune the selectivity of the products.[9] Despite the advantages of photothermal catalysis, it is pertinent to ask if using light directly rather than using thermocatalysis has the potential to further reduce the CO$_2$ footprint of CO$_2$ utilization.

Herein we address this question using reverse water–gas shift (RWGS) and Sabatier reactions as models with which to discuss the prospects of photothermal catalysis in net CO$_2$ reduction. We present equations, based on which the net CO$_2$ reduction in thermal and photothermal catalytic processes performed in batch and flow reactors can be calculated. Considering that light needs to be practically coupled to the thermal systems, in which the catalysts have to be uniformly illuminated, we imagine the implementation of an assembly of small-scale abiological plants resembling agricultural greenhouses where a group of biological plants accomplish photosynthesis either from lamps or sunlight.[10]

S. Wang, W. Pan, J. Zhao, Prof. W. Sun, Prof. D. Yang
State Key Laboratory of Silicon Materials
School of Materials Science and Engineering
Zhejiang University
Hangzhou, Zhejiang 310027, P. R. China
E-mail: sunnyway423@zju.edu.cn; mseyang@zju.edu.cn

A. A. Tountas, Prof. G. A. Ozin
Materials Chemistry and Nanochemistry Research Group
Solar Fuels Cluster
Departments of Chemistry
University of Toronto
Toronto, Ontario M5S 3H6, Canada
E-mail: gozin@chem.utoronto.ca

Prof. L. He
Institute of Functional Nano and Soft Materials (FUNSOM)
Jiangsu Key Laboratory for Carbon-Based Functional Materials and Devices
Soochow University
Suzhou, Jiangsu 215123, China

**ADVANCED
SCIENCE NEWS**
www.advancedsciencenews.com

**NANO · MICRO
small**
www.small-journal.com

The key process parameters in this scheme include CO_2 emission per kWh of electricity, CO_2 emission per mol of H_2, the conversion rate of CO_2, and the electricity to power the system, all considered to understand their relationship to net CO_2 reduction. On the basis of these calculations, possible routes towards negative CO_2 emission through photothermal catalysis are proposed.

2. Results and Discussion

2.1. Net CO₂ Emission in Batch Reactors

Carbon monoxide and methane are the two most common products from CO_2 reduction through RWGS and Sabatier reactions, respectively.[2b,c,11] Technically, they are easier to obtain as compared to many other hydrocarbons such as methanol and C_{2+} products, which are usually generated under moderately high pressure. As a result, the published works in the emerging field of photothermal catalysis have mainly focused on these two CO_2-derived products. Besides, carbon monoxide is the main source in the production of hydrocarbons and methanol, and methane is the main constituent of natural gas, thereby providing promising feedstocks for further technology development and downstream industrial chemical synthesis. This is the motivation for understanding the net CO_2 emission, denoted as M, associated with photothermally catalyzed RWGS and Sabatier reactions. The value of M equals the amount of emitted CO_2 after subtracting the consumed CO_2. The former mainly comes from energy consumption during the generation of electricity and hydrogen while the latter results from the transformation of CO_2 into CO and CH_4 by the RWGS and Sabatier reactions, respectively. When $M < 0$, net CO_2 reduction can be achieved.

The type of the reactor system is a vital factor of the CO_2 footprint, since how the reactants are fed determines the final energy consumption of a catalytic process.[12] Currently the reactors for heterogeneous CO_2 reduction can be classified into two major categories: the batch reactors, and the flow reactors. In this section, we first focus the analysis on the former.

Batch reactors are commonly used for the study of catalysis, in which the reactants can have full access to the catalyst to achieve high conversion efficiency. Moreover, the reaction pressure and phase of reactants are flexible. These features make batch reactors excellent vessels for CO_2 reduction. The disadvantage is that they require labor force to constantly charge and discharge reactants and products. When it comes to photothermal catalysis, net CO_2 emission for RWGS and Sabatier reactions and the hybrid of them ($M1$) on batch reactors can be influenced by several parameters including CO_2 emission per kWh of electricity (x_1 mol), CO_2 produced per mol of H_2 (x_2 mol), the power consumption of utilities (lamp: a kW, pump: b kW), reaction conditions (mass of the catalyst: m g; the long service time of the reactor: t h; light irradiation time in a cycle: t_1 h; the time of discharging gas with a pump in a cycle: t_2 h; the time of charging fresh gas reactants in a cycle: t_3 h), and catalyst performance (conversion rate of CO_2: c mol·g^{-1}·h^{-1}; selectivity of CO: s_1; selectivity of CH_4: s_2). $M1$ can be denoted as $M1_{kp}$ or $M1_{rs}$ depending on whether the H_2 feed is calculated

based on the kinetic parameters or reaction stoichiometry, respectively (Equations (12) and (14)). To be specific, $M1_{kp}$ was calculated based on the original feed amount of H_2 (n mol in a cycle) while $M1_{rs}$ was obtained from the practically consumed amount of H_2.

As for the net CO_2 emission by thermocatalysis ($M2$) for batch reactors, since light is not involved, it is mainly determined by the electric energy consumed by the heating module (Q_{total}) and the temperature (T) in addition to b, c, m, s_1, s_2, t_1, t_2, t_3, x_1, and x_2 as described above. Similarly, $M2$ could be denoted as $M2_{kp}$ and $M2_{rs}$ (Equations (13) and (15)) corresponding with the H_2 feed calculated based on the kinetic parameters and reaction stoichiometry, respectively.

Figure S1, Supporting Information, illustrates the major components, auxiliary equipment, and key parameters for a typical batch reactor. The relationship between M and the parameters introduced above can be specified through the step-by-step derivations as follows.

For batch reactors, the CO_2 emitted by a lamp (M_{lamp}) within t h:

$$M_{lamp} = \frac{ax_1t_1t}{t_1 + t_2 + t_3} \tag{1}$$

Note that t_1 represents the actual light irradiation time in a single cycle.

The CO_2 emitted by a pump (M_{pump}) within t h:

$$M_{pump} = \frac{bx_1t_2t}{t_1 + t_2 + t_3} \tag{2}$$

The CO_2 emitted by the heating modulate (M_{heat}) within t h for thermocatalysis can be described according to the sum of the electricity consumed during the one-time ramping stage to the target temperature T, and the electricity consumed during the long service time, t, to maintain the reactor at T:

$$Q_{total} = k_1T + b_1 + (k_2T + b_2)t \tag{3}$$

$$\text{Accordingly, } M_{heat} = Q_{total}\,x_1 \tag{4}$$

in which k_1 and b_1, and k_2 and b_2 are constants determined by a specific batch reactor, which can be measured experimentally.

The CO_2 emitted by the generation of H_2 based on the kinetic parameters, denoted as $M(H_2)_{kp}$, within t h:

$$M(H_2)_{kp} = \frac{nx_2t}{t_1 + t_2 + t_3} \tag{5}$$

In all the calculations for batch reactors, n represents the original feed amount of H_2 in a single cycle.

The CO_2 emitted by the generation of H_2 based on the reaction stoichiometry, denoted as $M(H_2)_{rs}$, within t h:

$$M(H_2)_{rs} = \frac{(s_1 + 4s_2)mcx_2t_1t}{t_1 + t_2 + t_3} \tag{6}$$

From the report by Wang et al., $c = 0.024$ mol·g^{-1}·h^{-1}, $m = 0.12$ g, $n = 0.0042$ mol, $s_1 = 1$, $s_2 = 0$, $t_1 = 0.5$ h, and t_2 and

ADVANCED
SCIENCE NEWS
www.advancedsciencenews.com

NANO · MICRO
small
www.small-journal.com

t_3 were both set to be 1/12 h.[13] In a single cycle, the amount of consumed H_2 equals $(s_1 + 4s_2)mct_1 = 0.0014$ mol. As can be seen, it was smaller than the original feed amount of H_2 in a single cycle (n) which equals 0.0042 mol. In this case, $M(H_2)_{kp} = 0.0063x_2t$, and $M(H_2)_{rs} = 0.00216x_2t$.

The CO_2 consumed during the catalytic CO_2 reduction process ($M_{con.}$) within t h:

$$M_{con.} = \frac{mct_1t}{t_1 + t_2 + t_3} \quad (7)$$

Note that mct_1 represents the actual conversion amount of CO_2 in a single cycle.

Therefore,

$$M1_{kp} = M_{lamp} + M_{pump} + M(H_2)_{kp} - M_{con.} \text{ (Photothermal catalysis)} \quad (8)$$

$$M2_{kp} = M_{heat} + M_{pump} + M(H_2)_{kp} - M_{con.} \text{ (Thermocatalysis)} \quad (9)$$

$$M1_{rs} = M_{lamp} + M_{pump} + M(H_2)_{rs} - M_{con.} \text{ (Photothermal catalysis)} \quad (10)$$

$$M2_{rs} = M_{heat} + M_{pump} + M(H_2)_{rs} - M_{con.} \text{ (Thermocatalysis)} \quad (11)$$

$$M1_{kp} = \frac{\left[(x_1a - mc)t_1 + nx_2 + bx_1t_2\right]t}{t_1 + t_2 + t_3} \quad (12)$$

$$M2_{kp} = \left(k_2x_1T + b_2x_1 + \frac{bx_1t_2 + nx_2 - mct_1}{t_1 + t_2 + t_3}\right)t + (k_1T + b_1)x_1 \quad (13)$$

$$M1_{rs} = \frac{\left\{\left[x_1a + (s_1x_2 + 4s_2x_2 - 1)mc\right]t_1 + bx_1t_2\right\}t}{t_1 + t_2 + t_3} \quad (14)$$

$$M2_{rs} = \left[k_2x_1T + b_2x_1 + \frac{bx_1t_2 + (s_1x_2 + 4s_2x_2 - 1)mct_1}{t_1 + t_2 + t_3}\right]t + (k_1T + b_1)x_1 \quad (15)$$

The derivatives of M in terms of t (dM/dt, representing net CO_2 emission rate) are shown as follows:

$$dM1_{kp}/dt = \frac{(x_1a - mc)t_1 + nx_2 + bx_1t_2}{t_1 + t_2 + t_3} \quad (16)$$

$$dM2_{kp}/dt = k_2x_1T + b_2x_1 + \frac{bx_1t_2 + nx_2 - mct_1}{t_1 + t_2 + t_3} \quad (17)$$

$$dM1_{rs}/dt = \frac{\left[x_1a + (s_1x_2 + 4s_2x_2 - 1)mc\right]t_1 + bx_1t_2}{t_1 + t_2 + t_3} \quad (18)$$

$$dM2_{rs}/dt = k_2x_1T + b_2x_1 + \frac{bx_1t_2 + (s_1x_2 + 4s_2x_2 - 1)mct_1}{t_1 + t_2 + t_3} \quad (19)$$

When dM/dt is negative, the process is actually consuming CO_2 overtime rather than emitting CO_2.

Calculations of CO_2 footprints using the equations above can be demonstrated with real cases. Q_{total} (Equation (3)) can be measured by monitoring the energy consumption by a reactor for a certain reaction scale. Figure S2, Supporting Information, shows a typical photothermal batch reactor in our laboratory that allows input of both light and heat, which consists of a 100 mL reactor tank and a temperature-controller. The electricity consumed by it during operation and under different temperatures was recorded from which the Q_{total} of our batch reactor was summarized (Equation (20) and Figure S3, Supporting Information).

$$Q_{total} = 0.00397T - 0.20484 + (0.000434857T - 0.0176)t \quad (20)$$

To continue the calculation demonstration, the power of a typical pump for degassing the batch reactor in our laboratory and the previously defined parameters derived from the paper of Wang et al. (Table S1, Supporting Information) were taken into account.[13] The new photothermal catalyst (black indium oxide), introduced in the study by Wang et al., reached an equilibrium temperature of 262 °C under 20 suns, at which a high conversion rate of 23882.75 $\mu mol \cdot g^{-1} \cdot h^{-1}$ was obtained.[13] Next, based on the analysis by Chen and co-workers, the values of x_1 and x_2 were set to be 11.04 (based on the 2014 average energy production in the US) and 0.481 (based on the value from steam methane reforming), respectively.[7] t_2 and t_3 were both set to 1/12 h for the following calculations. For a prolonged service life, a derivative of M in terms of t (net CO_2 emission rate) can be taken to simplify the calculations, in which the service time of the reacting system is no longer present in the final expression, and the constant electricity consumed during the initial ramping process would become zero after derivation, corresponding well with the fact that it is negligible compared to the electricity consumed for maintaining the target T for a very long time (Equations (16)–(19)). When the power of the lamp (a kW) is set to be 0.15, $dM1_{kp}/dt$, $dM1_{rs}/dt$, $dM2_{kp}/dt$, and $dM2_{rs}/dt$ will have numerical values, which equal 1.79, 1.79, 1.6, and 1.6, respectively. The equal values of dM_{kp}/dt and dM_{rs}/dt indicate that it would not be necessary to recycle the remaining unreacted hydrogen. Note that $dM(H_2)_{kp}/dt$ and $dM(H_2)_{rs}/dt$ equal 0.003 and 0.001, respectively, which are small in comparison to the value of dM/dt. Therefore, the CO_2 emission during the generation of H_2 is a negligible part of the overall net CO_2 emission rate when compared to other contributors. Moreover, the net CO_2 emission rate in the photothermal process is even higher than that of thermocatalysis.

To reduce CO_2 emission from the photothermal catalysis, employing an energy-saving lamp with a lower power could be an effective strategy. The relationship between $dM1_{kp}/dt$ and a was studied by setting a as a variable (Figure S4a, Supporting Information). Evidently, the net CO_2 emission rate from the photothermal catalysis increases monotonously with the power of the lamp, while that from the thermocatalysis remains as a constant since the lamp is not used. Notably, when the lamp power a is smaller than 0.127 kW, the value of $dM1_{kp}/dt$ would be lower than $dM2_{kp}/dt$ which means that the net amount of effluent CO_2 in a photothermal catalytic process is less than that in a thermocatalytic process with a relatively efficient lamp. However, a negative CO_2 emission still cannot be achieved even when the lamp is power-free.

**ADVANCED
SCIENCE NEWS**
www.advancedsciencenews.com

**NANO · MICRO
small**
www.small-journal.com

Since the facilities used in current catalytic systems are mostly powered by electricity, improving the energy conversion system to reduce CO_2 emission during the generation of electricity should be a potential route to realize net CO_2 reduction.[14] Moreover, the fraction of electricity generated by renewable sources is becoming more significant globally, which could further reduce the CO_2 emission from this process. As shown in Figure S5a, Supporting Information, when the value of x_1 (CO_2 emission per kWh of electricity) decreases, dM_{kp}/dt drops sharply. Net-zero CO_2 reduction would be almost achieved when x_1 approaches zero. Therefore, electricity produced from solar energy would be an excellent candidate for the purpose of reducing CO_2 emission. However, it should be noted that a nearly zero CO_2 emission for electricity generation might be unrealistic.

Catalyst performance is another key factor influencing net CO_2 emission. Transforming CO_2 into valuable products is a promising route to reduce CO_2 emission in which the conversion rate (c) is the critical parameter that would determine the final amount of effluent CO_2. The relationship between c and dM_{kp}/dt is displayed by **Figure 1**. Net-zero CO_2 emission is only achieved until c increases and approaches 20 mol·g^{-1}·h^{-1}, which is unreachable for most catalysts reported. Nevertheless, increasing the value of c is always favorable in that a catalytic process with a larger c can emit a much smaller amount of CO_2 than one with a smaller c. For photothermal catalysis, c mainly depends on the local temperature of the catalyst, which is contingent upon its photothermal conversion efficiency and illumination intensity. Therefore, a higher conversion rate can be achieved by utilizing photothermal materials (e.g., black silicon and plasmonic metals) and solar concentrators. The design of photothermal materials is vital for the improvement of catalytic performance. Light absorption property is a key parameter in photothermal conversion. For semiconductors, the light harvesting ability can be improved by introducing dopants, defects, sensitizers, upconversion materials, or plasmonic metals. Furthermore, the morphology and dispersion of metal nanoparticles could greatly influence the light absorption as well.[6a] Materials with excellent thermal insulation properties should be another potential candidate for photothermal catalysis. The combination of light

absorbers and insulation materials could provide a golden opportunity for the construction of well-performing photothermal catalysts. Notably, a number of ground-breaking achievements have been realized under the efforts of previous researchers, shedding light on the progress of photothermal catalytic CO_2 reduction (Table S2, Supporting Information). Again taking the parameters in the paper of Wang et al. (detailed previously) into account, when black In_2O_3 is used as the catalyst, a high equilibrium temperature of 262 °C was obtained under a 10-sun illumination. Consequently, the value of c could reach 0.024 mol·g^{-1}·h^{-1} at which $dM1_{kp}/dt$ equals 1.798 (left green dash line in Figure 1b).[13] If a catalyst with a higher photothermal conversion efficiency and an illumination with a higher intensity were used, the temperature of the catalyst would be further increased to a much higher level, for example, 1000 °C. In this case, a maximum value of c would approach 0.04 mol·g^{-1}·h^{-1}. However, the value of $dM1_{kp}/dt$ only drops a little to 1.796 which might be ascribed to the limited feed amount of CO_2 in the batch reactor (right green dash line in Figure 1b). Therefore, a higher pressure or more reasonable design of batch reactors might be good choices for pursuing a higher conversion rate of CO_2, but their potential in further reducing the CO_2 emission might seem not as significant as lowering the electricity consumed by the lamp.

In this regard, photothermal catalysis directly driven by solar energy in lieu of an electric lamp seems to have the most potential as a way to realize negative CO_2 emission. When sunlight is used (an 8 h per day is taken for demonstrative calculation) as the light source and c is set as a variable, net reduction of CO_2 can be already achieved when c approaches 6.3 mol·g^{-1}·h^{-1} which is only about one-third of the c required in the case driven by a 150W lamp (**Figure 2**). As a pump is indispensable for batch reactors, the supply of electricity is still necessary even when the generation of H_2 is CO_2 free and the illumination source is switched to sunlight, in which the net CO_2 reduction can be obtained when x_1 is smaller than 0.042 using the black indium catalyst reported by Wang et al. (Figure S5b inset, Supporting Information). Unfortunately, this is still unavailable with current energy conversion systems in most parts of the world. Taking the US as an example,
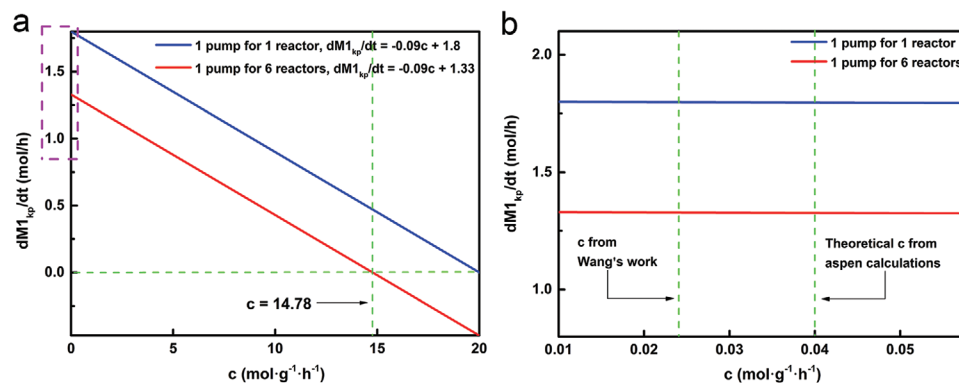

Figure 1. a) The dependence of net CO_2 reduction rate on the conversion rate of CO_2 (c) in a photothermal catalytic process driven by electricity-powered lamps for batch reactors. b) The enlarged graph of the enclosed area in (a). Theoretical c (conversion rate of CO_2: c mol·g^{-1}·h^{-1}) from aspen calculations described in (b) is calculated based on the maximal conversion rate in Figure S7, Supporting Information.

ADVANCED
SCIENCE NEWS
www.advancedsciencenews.com
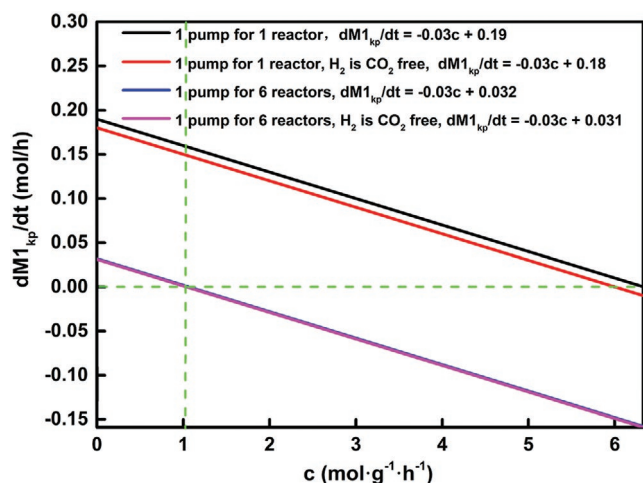
NANO · MICRO
small
www.small-journal.com

Figure 2. The dependence of net CO_2 reduction rate on the conversion rate of CO_2 in a photothermal catalytic process driven by sunlight for batch reactors when CO_2 emission per kWh of electricity (x_1) equals 11.04 mol (the 2014 average US energy production). A minimum c value of ≈ 1 mol g^{-1} h^{-1} is required to achieve net-zero CO_2 emission, marked by the dashed line.

the 2014 average energy production in US emitted 11.04 mol of CO_2 per kW h^{-1}, which is ≈ 263 times higher than this target value.[7] From these results, it seems that the pump for degassing actually contributed to a large part of the consumed electricity. For the 100-mL batch reactor used in our calculations, a 0.4-kW pump might be extravagant. Alternatively, if six reactors are supported by one pump, the total electricity consumption will be much smaller (Figures 1 and 2 and Figures S4 and S5, Supporting Information). Figure S6, Supporting Information, displays a blueprint of a model factory for batch reactors mimicking a greenhouse, in which the concentrators and reactors are close-packed to make the most use of space and light. Thanks to the reasonable reorganization of the reactors and pumps, net CO_2 reduction can be obtained with a smaller c of 14.78 mol·g^{-1}·h^{-1} under a 150-W lamp, compared with the previous value of 20 mol·g^{-1}·h^{-1} (Figure 1a). Notably, in a solar-powered process with the assumption that the generation of H_2 is CO_2 free, the value of c can further drop to 1 mol·g^{-1}·h^{-1} for the sake of a net-zero CO_2 reduction, which is realistic to achieve (Figure 2). Nevertheless, it is still very difficult to realize negative CO_2 emission by simply reducing x_1 while not increasing the catalyst performance, since a value as small as 0.26 is needed for x_1 even if one pump functions well with 6 reactors simultaneously, which is unachievable for the global energy structure in the near future (Figure S5b inset, Supporting Information).

2.2. Net CO$_2$ Emission in Flow Reactors

The flow reactor is another well-studied type of vessel for CO_2 hydrogenation reactions. Figure S8, Supporting Information, illustrates the major components, auxiliary equipment, and key parameters for a typical flow reactor. Operationally, it is much more convenient than batch reactors as there is no frequent degassing and purging

procedures. However, the conversion rate is limited due to the lessened contact between the reactants and the catalyst. Similar to batch reactors, the net emission of CO_2 for flow reactors can be calculated from Equations (21)–(38), specified through step-by-step derivations as follows, in which the characters represent the same parameters as described before, except that n now represents the feed rate of H_2 (unit: mol per hour). Accordingly, M_{kp} was calculated based on the original feed rate of H_2 while M_{rs} was obtained from the practically consumed rate of H_2.

The CO_2 emitted by a lamp (M_{lamp}) within t h:

$$M_{lamp} = a x_1 t \tag{21}$$

The CO_2 emitted by the heating modulate (M_{heat}) for thermocatalysis within t h:

$$Q_{total} = k_1 T + b_2 + (k_2 T + b_2) t \tag{22}$$

$$M_{heat} = Q_{total}\, x_1 \tag{23}$$

k_1 and k_2 are constants determined by a specific flow reactor.

The CO_2 emitted by the generation of H_2 based on the kinetic parameters, denoted as $M(H_2)_{kp}$, within t h:

$$M(H_2)_{kp} = n x_2 t \tag{24}$$

in which n represents the feed rate of H_2 (unit: mol per hour).

The CO_2 emitted by the generation of H_2 based on the reaction stoichiometry, denoted as $M(H_2)_{rs}$, within t h:

$$M(H_2)_{rs} = (s_1 + 4s_2) mct \tag{25}$$

The CO_2 consumed during the catalytic process ($M_{con.}$) within t h:

$$M_{con.} = mct \tag{26}$$

Therefore,

$$M1_{kp} = M_{lamp} + M(H_2)_{kp} - M_{con.} \tag{27}$$

$$M2_{kp} = M_{heat} + M(H_2)_{kp} - M_{con.} \tag{28}$$

$$M1_{rs} = M_{lamp} + M(H_2)_{rs} - M_{con.} \tag{29}$$

$$M2_{rs} = M_{heat} + M(H_2)_{rs} - M_{con.} \tag{30}$$

$$M1_{kp} = (x_1 a + n x_2 - mc) t \tag{31}$$

$$M2_{kp} = \left[(k_2 T + b_2) x_1 + n x_2 - mc \right] t + (k_1 T + b_1) x_1 \tag{32}$$

$$M1_{rs} = \left[x_1 a + (s_1 x_2 + 4 s_2 x_2 - 1) mc \right] t \tag{33}$$

$$M2_{rs} = \left[(k_2 T + b_2) x_1 + (s_1 x_2 + 4 s_2 x_2 - 1) mc \right] t + (k_1 T + b_1) x_1 \tag{34}$$

ADVANCED
SCIENCE NEWS
www.advancedsciencenews.com
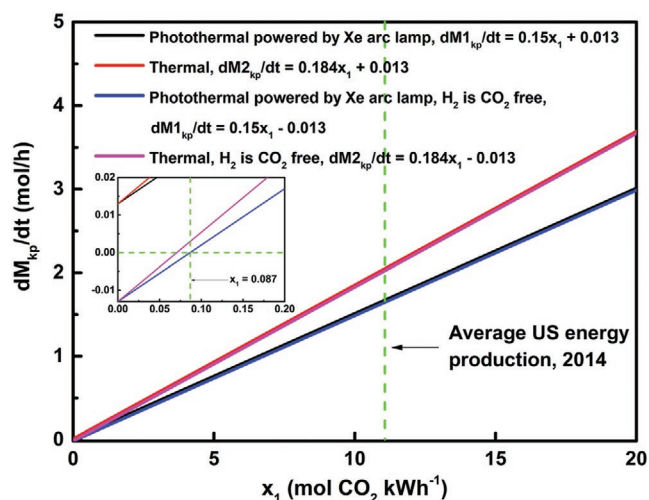
NANO · MICRO
small
www.small-journal.com

Figure 3. The dependence of net CO_2 reduction rate on CO_2 emission per kWh of electricity (x_1) for flow reactors. The lamp power was assumed to be 150 W. The dashed line in the inset shows the maximum x_1 which can achieve net CO_2 reduction.

The derivatives of M in terms of t are shown as follows:

$$dM1_{kp}/dt = x_1 a + nx_2 - mc \tag{35}$$

$$dM2_{kp}/dt = (k_2 T + b_2) x_1 + nx_2 - mc \tag{36}$$

$$dM1_{rs}/dt = x_1 a + (s_1 x_2 + 4s_2 x_2 - 1)mc \tag{37}$$

$$dM2_{rs}/dt = (k_2 T + b_2) x_1 + (s_1 x_2 + 4s_2 x_2 - 1)mc \tag{38}$$

Figure S9, Supporting Information, displays the outline and structural diagram of the flow reactor in our laboratory which is typical for thermo and photothermal catalysis. The electricity consumed by it at different temperatures for the thermocatalysis was recorded, based on which, Q_{total} of our flow reactor was summarized (Equation (39) and Figure S10, Supporting Information).

$$Q_{total} = 0.00222T - 0.1395 + (0.0004815T - 0.01601)t \tag{39}$$

Besides the power of our flow reactor, the relatively complete data and parameters of the catalytic system using Ru@FL-LDHs as an efficient photothermal catalyst (Table S3, Supporting Information) reported by Ye and co-workers were taken into account for the following discussions.[6g] When a is set to be 0.15 kW and x_1 is set as a variable, the net CO_2 emission rate is always lower by photothermal catalysis than that by thermocatalysis (**Figure 3**), which is contrary to the situation in batch reactors. This might be ascribed to the higher power consumed in the heating module and more available time for light illumination for the flow reactors than for the batch ones. The usage of energy-saving lamps to reduce a can efficiently reduce $dM1_{kp}/dt$ as well (Figure S11, Supporting Information). The usage of a lamp with a higher power should be avoided as the net CO_2 emission rate of the photothermal

process will exceed that of a thermal process when the value of a is larger than 0.18 kW.

Conversion rate plays an important role in reducing CO_2 emission for flow reactors (**Figure 4**). To realize net CO_2 reduction, a high conversion rate of at least 11.2 $mol \cdot g^{-1} \cdot h^{-1}$ is necessary which is almost impossible to achieve with the existing catalysts (Figure 4a). When sunlight is used as the light source, the value can drop sharply to 0.176 $mol \cdot g^{-1} \cdot h^{-1}$. It seems that CO_2 emitted during the generation of H_2 has a much lesser effect on the final amount of effluent CO_2 compared to that caused by the electricity consumed by the lamp. However, for the sunlight-driven process, it still matters especially when the value of c is small for which the value of $dM1_{kp}/dt$ is still positive for the CO_2-emitted H_2 generation process (Figure 4b). Notably, negative CO_2 emission can always be achieved when the generation of H_2 is CO_2-free, which might be through water splitting driven by sustainable power sources.[15] The maximum conversion efficiency of CO_2 was also calculated from Aspen Plus V9. Apparently, for the Sabatier reaction and a relatively low temperature (e.g., below 250 °C) total conversion of CO_2 when the feed ratio of CO_2:H_2 equals 1:4 is theoretically achievable (Figure S12, Supporting Information). This indicates there is still great potential in further improving the catalyst performance in a flow reactor in order to reduce the CO_2 footprint.

3. Conclusion

Photothermal catalytic CO_2 reduction is a potential route to realizing negative CO_2 emission. The CO_2 footprint associated with the process is influenced by performance factors including CO_2 emission per kWh of electricity generated, CO_2 emission per mol of H_2 generated, the conversion rate of CO_2, and the power consumption by equipment (e.g., lamp, heating elements, and pump). It is imperative to develop energy-saving lamps for the sake of reducing CO_2 emission and replacing traditional thermocatalysis. For batch reactors in our cases, only lamps with a power less than 0.12 kW can likely make a photothermal catalytic process more favorable than a thermocatalytic one. Reasonable resource and facility management, such as multiple reactors powered by a single pump, greatly reduce the overall electricity consumption. Undoubtedly, it is much easier to realize net CO_2 reduction by using sunlight or electricity from green energy as the power source in which a CO_2 conversion rate at the level of about 1 $mol \cdot g^{-1} \cdot h^{-1}$ is adequate. It seems that flow reactors have more advantages than batch ones, since a much lower CO_2 conversion rate at the level of 0.176 $mol \cdot g^{-1} \cdot h^{-1}$ is feasible for net CO_2 reduction when sunlight is utilized as the energy source. Nevertheless, it is still very hard to achieve this rate and high CO_2 conversion efficiency simultaneously. It is encouraging that a negative CO_2 emission is always available when the feed H_2 is CO_2-cost-free for a solar-powered photothermal catalytic process. Overall, there might exist some restrictions for the results of the examples in this study. Nevertheless, the equations and preliminary data presented should provide a valuable guide for the future development of photothermal catalysis for CO_2 reduction.
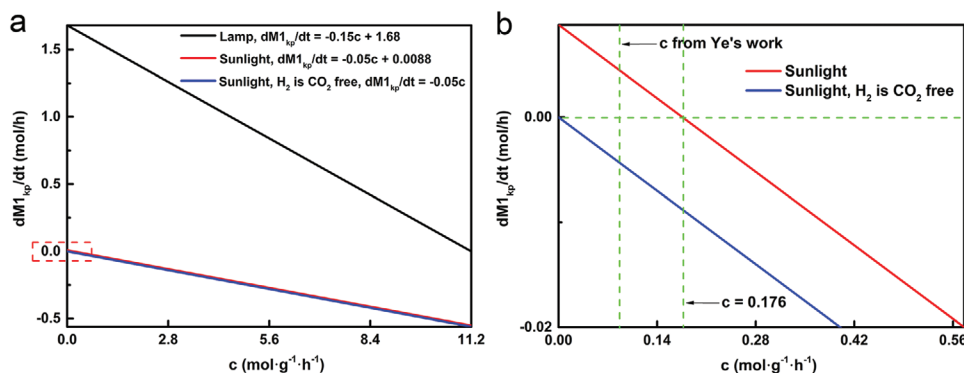
Figure 4. a) The dependence of net CO_2 reduction rate on the conversion rate of CO_2 (c) for flow reactors. b) The enlarged graph of the enclosed area in (a). A minimum c value of ≈ 0.176 mol g^{-1} h^{-1} is required to achieve net-zero CO_2 emission for the photothermal catalysis driven by sunlight and industrially produced H_2, marked by the dashed line. Whereas when H_2 is considered CO_2-free, CO_2 emission is always negative.

4. Experimental Section

In all sunlight-driven cases, the sunshine duration was set to be 8 h per day. For simplicity, the gas compression and separation process were not considered.

Supporting Information

Supporting Information is available from the Wiley Online Library or from the author.

Acknowledgements

Conflict of Interest

The authors declare no conflict of interest.

Keywords

[1] a) P. L. Munday, D. L. Dixson, M. J. Welch, D. P. Chivers, P. Domenici, M. Grosell, R. M. Heuer, G. P. Jones, M. I. McCormick, M. Meekan, G. E. Nilsson, T. Ravasi, S.-A. Watson, *Nature* **2020**, *586*, E20; b) X. Jiang, X. Nie, X. Guo, C. Song, J. G. Chen, *Chem. Rev.* **2020**, *120*, 7984; c) N. Gruber, D. Clement, B. R. Carter, R. A. Feely, S. van Heuven, M. Hoppema, M. Ishii, R. M. Key, A. Kozyr, S. K. Lauvset, C. L. Monaco, J. T. Mathis, A. Murata, A. Olsen, F. F. Perez, C. L. Sabine, T. Tanhua, R. Wanninkhof, *Science* **2019**, *363*, 1193; d) L. Zhang, Z.-J. Zhao, T. Wang, J. Gong, *Chem. Soc. Rev.* **2018**, *47*, 5423.

[2] a) C. Vogt, E. Groeneveld, G. Kamsma, M. Nachtegaal, L. Lu, C. J. Kiely, P. H. Berben, F. Meirer, B. M. Weckhuysen, *Nat. Catal.* **2018**, *1*, 127; b) M. Juneau, M. Vonglis, J. Hartvigsen, L. Frost, D. Bayerl, M. Dixit, G. Mpourmpakis, J. R. Morse, J. W. Baldwin, H. D. Willauer, M. D. Porosoff, *Energy Environ. Sci.* **2020**, *13*, 2524; c) X. Li, Y. Sun, J. Xu, Y. Shao, J. Wu, X. Xu, Y. Pan, H. Ju, J. Zhu, Y. Xie, *Nat. Energy* **2019**, *4*, 690.

[3] a) F. G. Baddour, E. J. Roberts, A. T. To, L. Wang, S. E. Habas, D. A. Ruddy, N. M. Bedford, J. Wright, C. P. Nash, J. A. Schaidle, R. L. Brutchey, N. Malmstadt, *J. Am. Chem. Soc.* **2020**, *142*, 1010; b) Y. Wang, S. Kattel, W. Gao, K. Li, P. Liu, J. G. Chen, H. Wang, *Nat. Commun.* **2019**, *10*, 1166.

[4] a) C. Choi, S. Kwon, T. Cheng, M. Xu, P. Tieu, C. Lee, J. Cai, H. M. Lee, X. Pan, X. Duan, W. A. Goddard, Y. Huang, *Nat. Catal.* **2020**, *3*, 804; b) W. Ma, S. Xie, T. Liu, Q. Fan, J. Ye, F. Sun, Z. Jiang, Q. Zhang, J. Cheng, Y. Wang, *Nat. Catal.* **2020**, *3*, 478; c) A. Wagner, C. D. Sahm, E. Reisner, *Nat. Catal.* **2020**, *3*, 775; d) M. Li, H. Wang, W. Luo, P. C. Sherrell, J. Chen, J. Yang, *Adv. Mater.* **2020**, *32*, 2001848; e) J. A. Rabinowitz, M. W. Kanan, *Nat. Commun.* **2020**, *11*, 5231; f) R.-B. Song, W. Zhu, J. Fu, Y. Chen, L. Liu, J.-R. Zhang, Y. Lin, J.-J. Zhu, *Adv. Mater.* **2020**, *32*, 1903796; g) Q. Yang, Q. Wu, Y. Liu, S. Luo, X. Wu, X. Zhao, H. Zou, B. Long, W. Chen, Y. Liao, L. Li, P. K. Shen, L. Duan, Z. Quan, *Adv. Mater.* **2020**, *32*, 2002822; h) Y. Zhou, R. Zhou, X. Zhu, N. Han, B. Song, T. Liu, G. Hu, Y. Li, J. Lu, Y. Li, *Adv. Mater.* **2020**, *32*, 2000992; i) Y. Liu, D. Tian, A. N. Biswas, Z. Xie, S. Hwang, J. H. Lee, H. Meng, J. G. Chen, *Angew. Chem., Int. Ed.* **2020**, *59*, 11345; j) Q. He, D. Liu, J. H. Lee, Y. Liu, Z. Xie, S. Hwang, S. Kattel, L. Song, J. G. Chen, *Angew. Chem., Int. Ed.* **2020**, *59*, 3033; k) J. H. Lee, S. Kattel, Z. Jiang, Z. Xie, S. Yao, B. M. Tackett, W. Xu, N. S. Marinkovic, J. G. Chen, *Nat. Commun.* **2019**, *10*, 3724; l) W. Luc, B. H. Ko, S. Kattel, S. Li, D. Su, J. G. Chen, F. Jiao, *J. Am. Chem. Soc.* **2019**, *141*, 9902; m) J. Wang, S. Kattel, C. J. Hawxhurst, J. H. Lee, B. M. Tackett, K. Chang, N. Rui, C.-J. Liu, J. G. Chen, *Angew. Chem., Int. Ed.* **2019**, *58*, 6271; n) Y. He, Y. Li, J. Zhang, S. Wang, D. Huang, G. Yang, X. Yi, H. Lin, X. Han, W. Hu, Y. Deng, J. Ye, *Nano Energy* **2020**, *77*, 105010; o) W. Zhu,

L. Zhang, S. Liu, A. Li, X. Yuan, C. Hu, G. Zhang, W. Deng, K. Zang, J. Luo, Y. Zhu, M. Gu, Z.-J. Zhao, J. Gong, *Angew. Chem., Int. Ed.* **2020**, *59*, 12664; p) W. Zhu, L. Zhang, P. Yang, X. Chang, H. Dong, A. Li, C. Hu, Z. Huang, Z.-J. Zhao, J. Gong, *Small* **2018**, *14*, 1703314; q) W. Deng, L. Zhang, L. Li, S. Chen, C. Hu, Z.-J. Zhao, T. Wang, J. Gong, *J. Am. Chem. Soc.* **2019**, *141*, 2911.

[5] a) Y. F. Li, W. Lu, K. Chen, P. Duchesne, A. Jelle, M. Xia, T. E. Wood, U. Ulmer, G. A. Ozin, *J. Am. Chem. Soc.* **2019**, *141*, 14991; b) U. Ulmer, T. Dingle, P. N. Duchesne, R. H. Morris, A. Tavasoli, T. Wood, G. A. Ozin, *Nat. Commun.* **2019**, *10*, 3169; c) W. Sun, X. Yan, C. Qian, P. N. Duchesne, S. G. Hari Kumar, G. A. Ozin, *Faraday Discuss.* **2020**, *222*, 424; d) G. Xu, H. Zhang, J. Wei, H.-X. Zhang, X. Wu, Y. Li, C. Li, J. Zhang, J. Ye, *ACS Nano* **2018**, *12*, 5333; e) S. Wang, X. Hai, X. Ding, S. Jin, Y. Xiang, P. Wang, B. Jiang, F. Ichihara, M. Oshikiri, X. Meng, Y. Li, W. Matsuda, J. Ma, S. Seki, X. Wang, H. Huang, Y. Wada, H. Chen, J. Ye, *Nat. Commun.* **2020**, *11*, 1149; f) F. Chen, Z. Ma, L. Ye, T. Ma, T. Zhang, Y. Zhang, H. Huang, *Adv. Mater.* **2020**, *32*, 1908350; g) X. Xiong, Y. Zhao, R. Shi, W. Yin, Y. Zhao, G. I. N. Waterhouse, T. Zhang, *Sci. Bull.* **2020**, *65*, 987; h) L. Liu, H. Huang, F. Chen, H. Yu, N. Tian, Y. Zhang, T. Zhang, *Sci. Bull.* **2020**, *65*, 934; i) T. Wang, J. Gong, *Nat. Energy* **2020**, *5*, 642; j) A. Li, Q. Cao, G. Zhou, B. V. K. J. Schmidt, W. Zhu, X. Yuan, H. Huo, J. Gong, M. Antonietti, *Angew. Chem., Int. Ed.* **2019**, *58*, 14549; k) A. Li, T. Wang, C. Li, Z. Huang, Z. Luo, J. Gong, *Angew. Chem., Int. Ed.* **2019**, *58*, 3804; l) L. He, T. E. Wood, B. Wu, Y. C. Dong, L. B. Hoch, L. M. Reyes, D. Wang, C. Kubel, C. X. Qian, J. Jia, K. Liao, P. G. O'Brien, A. Sandhel, J. Y. Y. Loh, P. Szymanski, N. P. Kherani, T. C. Sum, C. A. Mims, G. A. Ozin, *ACS Nano* **2016**, *10*, 5578.

[6] a) K. Feng, S. H. Wang, D. K. Zhang, L. Wang, Y. Y. Yu, K. Feng, Z. Li, Z. J. Zhu, C. R. Li, M. J. Cai, Z. Y. Wu, N. Kong, B. H. Yan, J. Zhong, X. H. Zhang, G. A. Ozin, L. He, *Adv. Mater.* **2020**, *32*, 2000014; b) C. X. Qian, W. Sun, D. L. H. Hung, C. Y. Qiu, M. Makaremi, S. G. H. Kumar, L. L. Wan, M. Ghoussoub, T. E. Wood, M. K. Xia, A. A. Tountas, Y. F. Li, L. Wang, Y. C. Dong, I. Gourevich, C. V. Singh, G. A. Ozin, *Nat. Catal.* **2019**, *2*, 46; c) W. Sun, C. X. Qian, L. He, K. K. Ghuman, A. P. Y. Wong, J. Jia, A. A. Jelle, P. G. O'Brien, L. M. Reyes, T. E. Wood, A. S. Helmy, C. A. Mims, C. V. Singh, G. A. Ozin, *Nat. Commun.* **2016**, *7*, 12553; d) Z.-j. Wang, H. Song,

H. Liu, J. Ye, *Angew. Chem., Int. Ed.* **2020**, *59*, 8016; e) G. Liu, X. Meng, H. Zhang, G. Zhao, H. Pang, T. Wang, P. Li, T. Kako, J. Ye, *Angew. Chem., Int. Ed.* **2017**, *56*, 5570; f) S. Ning, H. Xu, Y. Qi, L. Song, Q. Zhang, S. Ouyang, J. Ye, *ACS Catal.* **2020**, *10*, 4726; g) J. Ren, S. Ouyang, H. Xu, X. Meng, T. Wang, D. Wang, J. Ye, *Adv. Energy Mater.* **2017**, *7*, 1601657; h) L. Wan, Q. Zhou, X. Wang, T. E. Wood, L. Wang, P. N. Duchesne, J. Guo, X. Yan, M. Xia, Y. F. Li, A. A. Jelle, U. Ulmer, J. Jia, T. Li, W. Sun, G. A. Ozin, *Nat. Catal.* **2019**, *2*, 889; i) D. Zhang, K. Lv, C. Li, Y. Fang, S. Wang, Z. Chen, Z. Wu, W. Guan, D. Lou, W. Sun, D. Yang, L. He, X. Zhang, *Sol. RRL* **2020**, *5*, 2000387.

[7] B. M. Tackett, E. Gomez, J. G. Chen, *Nat. Catal.* **2019**, *2*, 381.

[8] X. Meng, T. Wang, L. Liu, S. Ouyang, P. Li, H. Hu, T. Kako, H. Iwai, A. Tanaka, J. Ye, *Angew. Chem., Int. Ed.* **2014**, *53*, 11478.

[9] D. Mateo, J. L. Cerrillo, S. Durini, J. Gascon, *Chem. Soc. Rev.* **2021**, *50*, 2173.

[10] R. Dittmeyer, M. Klumpp, P. Kant, G. Ozin, *Nat. Commun.* **2019**, *10*, 1818.

[11] a) S. Farsi, W. Olbrich, P. Pfeifer, R. Dittmeyer, *Chem. Eng. J.* **2020**, *388*, 124233; b) H. Kirsch, U. Sommer, P. Pfeifer, R. Dittmeyer, *Chem. Eng. Sci.* **2020**, *227*, 115930; c) R. Shi, J. Guo, X. Zhang, G. I. N. Waterhouse, Z. Han, Y. Zhao, L. Shang, C. Zhou, L. Jiang, T. Zhang, *Nat. Commun.* **2020**, *11*, 3028; d) X. L. Yan, W. Sun, L. M. Fan, P. N. Duchesne, W. Wang, C. Kubel, D. Wang, S. G. H. Kumar, Y. F. Li, A. Tavasoli, T. E. Wood, D. L. H. Hung, L. L. Wan, L. Wang, R. Song, J. L. Guo, I. Gourevich, A. A. Jelle, J. J. Lu, R. F. Li, B. D. Hatton, G. A. Ozin, *Nat. Commun.* **2019**, *10*, 11.

[12] H. Wang, J. Jia, L. Wang, K. Butler, R. Song, G. Casillas, L. He, N. P. Kherani, D. D. Perovic, L. Jing, A. Walsh, R. Dittmeyer, G. A. Ozin, *Adv. Sci.* **2019**, *6*, 1902170.

[13] L. Wang, Y. Dong, T. Yan, Z. Hu, A. A. Jelle, D. M. Meira, P. N. Duchesne, J. Y. Y. Loh, C. Qiu, E. E. Storey, Y. Xu, W. Sun, M. Ghoussoub, N. P. Kherani, A. S. Helmy, G. A. Ozin, *Nat. Commun.* **2020**, *11*, 2432.

[14] R. G. Grim, Z. Huang, M. T. Guarnieri, J. R. Ferrell, L. Tao, J. A. Schaidle, *Energy Environ. Sci.* **2020**, *13*, 472.

[15] B. Parkinson, P. Balcombe, J. F. Speirs, A. D. Hawkes, K. Hellgardt, *Energy Environ. Sci.* **2019**, *12*, 19.